J Biol Phys (2013) 39:301–325
DOI 10.1007/s10867-013-9314-z

ORIGINAL PAPER

Design rules for nanomedical engineering: from physical virology to the applications of virus-based materials in medicine

Amy M. Wen · Pooja H. Rambhia · Roger H. French · Nicole F. Steinmetz

Received: 2 January 2013 / Accepted: 7 February 2013 / Published online: 19 April 2013

Abstract Physical virology seeks to define the principles of physics underlying viral infections, traditionally focusing on the fundamental processes governing virus assembly, maturation, and disassembly. A detailed understanding of virus structure and assembly has facilitated the development and analysis of virus-based materials for medical applications. In this *Physical Virology* review article, we discuss the recent developments in nanomedicine that help us to understand how physical properties affect the *in vivo* fate and clinical impact of (virus-based) nanoparticles. We summarize and discuss the design rules that need to be considered for the successful development and translation of virus-based nanomaterials from bench to bedside.

Keywords Design rules · Viral nanoparticles · Physical virology · Nanotechnology · Nanomedicine · Drug delivery · Long range interactions

A. M. Wen
Department of Biomedical Engineering, School of Engineering, Case Western Reserve University, Cleveland, OH 44106, USA

N. F. Steinmetz
Department of Biomedical Engineering, School of Medicine, Case Western Reserve University, Cleveland, OH 44106, USA

P. H. Rambhia
Department of Biochemistry, School of Medicine, Case Western Reserve University, Cleveland, OH 44106, USA

R. H. French · N. F. Steinmetz
Materials Science and Engineering, School of Engineering, Case Western Reserve University, 10900 Euclid Avenue, Cleveland, OH 44106, USA

N. F. Steinmetz (✉)
Department of Radiology, School of Medicine, Case Western Reserve University, Cleveland, OH 44106, USA
e-mail: nicole.steinmetz@case.edu

1 Introduction: virus-based materials in medicine

Nanomedicine is an attractive field of research because it offers the potential for noninvasive diagnosis and treatment options. Nanoparticles are advantageous because their large surface-area-to-volume ratio allows functionalization with payloads of targeting ligands to ensure tissue-specific delivery, labels for tracking or disease imaging, and drugs for therapy [1]. Nanoparticles are used to partition cargos between diseased and healthy tissue, ideally avoiding healthy tissues or at least minimizing the accumulation of toxic substances in healthy organs [2]. Several classes of nanomaterials are currently undergoing preclinical/clinical development and testing, including dendrimers, liposomes, polymers, metallic nanoparticles, and viral nanoparticles (VNPs). Each class offers distinct advantages and disadvantages in terms of functionality, physiochemical properties, biodistribution, pharmacokinetic behavior, immunogenicity, and toxicity:

- *Dendrimers* are inexpensive and easy to manufacture, but some are not biocompatible [3, 4].
- *Metallic nanoparticles* have physiochemical properties that make them useful for imaging and therapeutic applications, but some formulations show slow tissue clearance [5].
- *Polymers* and *liposomes* are biodegradable and nontoxic, but are prone to degradation *in vivo* [6, 7]. Their large size (>100 nm) also hinders tissue penetration and effective distribution [1].
- *Viral nanoparticles* (VNPs) come in different shapes and sizes and are tunable with atomic precision. However, like other protein-based nanomaterials, they are immunogenic. Strategies such as PEGylation can be used to overcome the immunogenicity of VNPs [8–13].

The development and application of virus-based materials in medicine is a growing field with a strong potential impact [14–16]. There are many novel types of VNPs under development, with those based on bacteriophages and plant viruses favored because they are considered safer in humans than mammalian viruses [17]. Preclinical studies in mice have shown that plant viruses can be administered at doses of up to 100 mg (10^{16} VNPs) per kilogram body weight without signs of toxicity [18, 19]. In contrast, 10^{11} adenovirus particles can cause severe hepatoxicity [20]. VNPs are also advantageous because genetic engineering allows (at least theoretically) the introduction of precise and reproducible modifications so that large quantities of identical particles matched to individual patient disease profiles can be manufactured as personalized medicines. VNPs are genetically encoded and self-assemble into discrete and monodisperse structures with a precise shape and size (Fig. 1). Virus structures are understood at atomic resolution, and self-assembly of mutant and chimeric particles has been established for a number of viral systems, allowing the development of protocols for high-precision VNP tailoring. This level of quality control cannot yet be achieved with synthetic nanoparticles. This unique vector system can also be combined with chemical modifications to add further functionality. Finally, the production of plant viruses or bacteriophages using molecular farming in plants or fermentation in cells is highly scalable and economical.

VNPs come in many shapes and sizes (Fig. 1). As with other nanomaterials, the vast majority of VNPs in research and development are spherical (i.e., icosahedral), e.g., adenovirus-based gene-delivery vectors and plant viruses such as *Cowpea mosaic virus* (CPMV), *Brome mosaic virus* (BMV), *Cowpea chlorotic mottle virus* (CCMV), *Hibiscus chlorotic ringspot virus* (HCRSV), and *Red clover necrotic mottle virus* (RCNMV) [18, 23–32]. A few high-aspect-ratio virus-based materials have also been investigated, principally *Tobacco mosaic virus* (TMV), *Potato virus X* (PVX), and bacteriophage M13 [33–36].

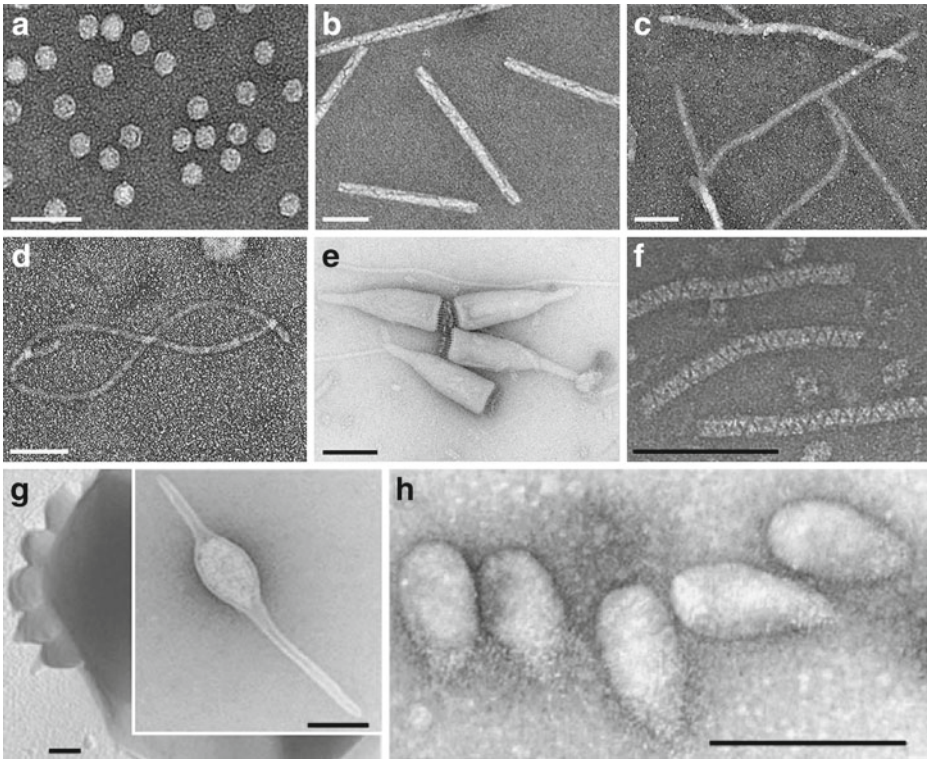

Fig. 1 Transmission electron micrographs of the following viruses: **a** Icosahedral cowpea mosaic virus. **b** Rod-shaped tobacco mosaic virus. **c** Filamentous potato virus X. **d** Highly flexible grapevine virus A (a single GVA particle is shown). **e** *Acidianus* bottle-shaped virus. Reproduced with permission from Praghisvili et al. Nature Reviews 2006 [21]. **f** *Acidianus* zipper-like virus. Reproduced with permission from Rachel et al., Arch Virol 2002 [22]. **g** Acidianius two-tailed virus and its extrusion from the host cell. Reproduced with permission from Praghisvili et al. Nature Reviews 2006 [21]. **h** *Sulfolobus neozealandicus* droplet-shaped virus. Reproduced with permission from Praghisvili et al., Nature Reviews 2006 [21]. *Scale bars* are 100 nm

2 Design rules in nanomedical engineering

Recent research has investigated the effect of shape, size, charge, and other surface characteristics on the behavior of nanoparticles within the body. Rules are now emerging to guide the design of nanoparticle-based therapeutics and diagnostics for *in vivo* applications. Nevertheless, untangling the interplay between the surface chemistry, size, and charge of nanoparticles and the complex biological barriers encountered en route to target tissues remains an exciting challenge. Biophysical modeling focused on the fundamental interactions at play coupled with both *in vitro* and *in vivo* experiments have begun to shed light on these factors and their role in cellular uptake, vascular interactions, passive and active targeting, and biodistribution.

Long-range interactions (LRIs) play an important role in biological, physical, and chemical processes and were the focus of a recent U.S. Department of Energy, Office of Science workshop and review [37] spanning the biology, chemistry, and physics communities. LRIs are categorized as being long-range electrodynamic, electrostatic, and polar

interactions that dominate the organization of small objects at separations beyond an interatomic bond length. They give rise to forces that help systems lower their thermodynamic free energy. They should be distinguished from the basic chemical process of covalent bond formation associated with chemical reactions, and the basic biological processes of metabolism leading to energy production. In addition, more than a dozen "different" LRIs are typically defined and used by researchers in particular scientific fields, e.g., hydrophobic [38], hydration, steric, depletion, and other interactions [39]. The impact of these types of particularization in LRIs is closely tied to specific application areas, which while convenient in the subfields, is an inhibition of the fundamental advancement in the nanoscale science of long-range interactions. For example, the van der Waals-London dispersion interactions and Casimir interactions are identically electrodynamic LRIs. These particular cases of LRIs, useful in their respective subfields, can at the same time be considered fundamentally from their origins, as combinations of the three fundamental LRIs: the electrodynamic van der Waals-London dispersion (vdW–Ld) interaction, the Coulombic or electrostatic interaction of importance in systems with net-charged moieties, and polar or acid-base interactions. This emphasis on the fundamental LRIs will help clarify and advance the field of LRIs and their broad role across the fields of science. These interactions have differing interaction lengths, all greater than simple covalent bond lengths, and differing relative magnitudes, but they all can play critical roles in the behavior of complex heterogenous systems. These are the class of systems that are critical in nanomedical engineering, where we strive to design nanomedicine vehicles that can be assembled, transported through the circulatory system, and ultimately disassemble in the diseased cells after leaving the circulatory system. Therefore, the three LRIs at play turn out to be important contributors to the mesoscale challenge of nanomedicine, producing vehicles with controlled lifetime performance from fabrication to delivery and beneficial impact at the target site.

Translational research involving VNPs is gaining momentum, including the development of VNPs for applications in drug and siRNA delivery as well as positron emission tomography (PET) and magnetic resonance (MR) imaging [40]. There are currently approximately 20 different platforms under investigation; a consensus on overall performance has yet to be reached. Recent studies have yielded general principles and models that have been applied specifically to the development and application of VNPs. These exciting new research initiatives have revealed certain differences in both the behavior and properties of icosahedral, rod-like, and filamentous viruses, providing tools for further investigation. Together, these studies lay the foundation for the intelligent design of nanoparticles with the ideal combination of properties for specific medical applications. As we forge the foundational connection between biomedical engineering and biological physics, so as to understand the three LRIs and the chemical and biological processes that determine the lifecycle of nanomedicines in the body, we will be able to address and optimize their efficacy.

3 Nanoparticle–cell interactions

Nanoparticles face various biological barriers en route to their target site; the first hurdle is the circulatory system with its complex composition of plasma proteins and immune cells specialized to remove foreign materials form circulation. Surface chemistries and geometry of the nanocarrier are variables to be tailored to minimize undesired cell interaction with non-target cells. Once at the target site, cell targeting and uptake into diseased cells are desired for effective cargo delivery; again surface chemistry and geometry

are variables that determine cell uptake interactions. To be successful in drug delivery, a balance between shielding from circulatory cells and targeting of disease cells must be accomplished.

In aqueous biological systems containing cells and nanoparticles, there are similarities to the colloidal chemistry of aqueous particulate systems in which one considers the attractive and repulsive particle interactions [41]. The electrodynamic vdW–Ld interaction is universal, present in all systems, and serves to set a comparative scale or magnitude for the intermolecular or interparticle force balance, which may be increased or decreased through the contributions of other LRIs. These vdW–Ld interactions in combination with electrostatic and polar interactions produce a rich range of behavior that encompasses stable dispersions and long circulation times, all the way to attractions that lead to flocculation and the removal of particles from the fluid phase.

3.1 Phagocytosis of nanoparticles

3.1.1 Phagocytosis: the impact of particle shape

Phagocytosis is a cellular process involving the uptake of specific targets into cells, which mediates several key functions of the human innate immune system including the clearance of pathogens and senescent cells [42]. Phagocytosis also removes nanomaterials from the circulation and deposits them in non-target organs, which is a significant challenge in nanomedicine. For many nanoparticle formulations, only a fraction of the injected dose will reach the target tissue, whereas the majority will accumulate in the liver and spleen [43]. Understanding the phagocytosis of nanomaterials is thus a key step in nanomedical engineering because avoiding phagocytosis is a stepping-stone to effective drug delivery.

Although the uptake mechanism used by immune cells such as macrophages is well characterized, the impact of target geometry remains elusive. The effect of target size and shape on phagocytosis has been investigated using a variety of model polystyrene targets [44]. Time-lapse video microscopy revealed that particle internalization relies on local particle shape at the initial point of contact with the macrophage, but not particle size. Shape-dependence was quantified using the contact angle (Ω), defined as the angle between the cell membrane and the average direction of tangents along the contour of the target (Fig. 2) [44]. There was a negative relationship between the rate of phagocytosis and Ω, where macrophage attachment to targets along the major axis (small Ω) allowed rapid internalization, whereas attachment along the minor axis ($\Omega > 45°$) prevented internalization but allowed spreading over the target. Further investigation into the underlying mechanism showed that actin cup formation was effectively inhibited by attachment along the minor axis. Thus, shape was shown to affect the initiation of internalization, whereas size may make the difference between the completion and cancellation of uptake [44].

Similar observations were reported when worm-like filomicelles were taken up by phagocytosis. The efficiency of phagocytosis was reduced as the aspect ratio of the filomicelles increased under static conditions [45]. This probably reflects the reduced likelihood of macrophage attachment along the major axis for the longer particles. Furthermore, macrophages under flow conditions did not internalize the longer filomicelles as readily due to the alignment and extension of the filaments in the flow field [45].

One of the fundamental aspects of these fluid–solid interactions is wetting, and can be seen in the contact angle of a fluid droplet on a surface or membrane [46, 47]. The nature of

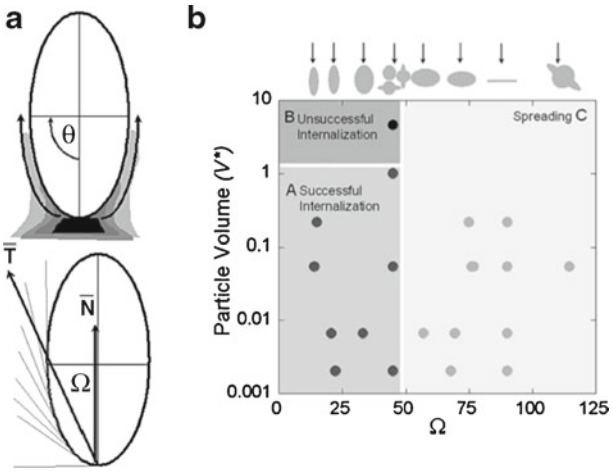

Fig. 2 **a** Definition of Ω and its relationship with membrane velocity. A schematic diagram illustrating how membrane progresses tangentially around elliptical disks. T represents the average of tangential angles from $\theta = 0$ to $\theta = \Pi/2$. Ω is the angle between T and membrane normal at the site of attachment, N. **b** Phagocytosis phase diagram with Ω and dimensionless particle volume V* (particle volume divided by 7.5 μm radius spherical cell volume) as governing parameters ($n = 5$ for each point). Initialization of internalization is judged by the presence of an actin cup or ring. There are three regions. Cells attaching to particles at areas of high $\Omega > 45°$, spread but do not initiate internalization (region C). Cells attaching to particles at areas of low $\Omega < 45°$, initiate internalization (regions A and B). If V* is ≤ 1, internalization is completed (region A). If $V^* > 1$, internalization is not completed because of the size of the particle (region B). The *arrows above the plot* indicate the point of attachment for each shape that corresponds to the value of Ω on the x-axis. Each case was classified as phagocytosis or no phagocytosis if >95% of observations were consistent. Each *data point* represents a different shape, size, or aspect ratio particle. Reproduced with permission from Champion et al., PNAS 2006 [44]

the fluid also changes the contact angle dramatically, as for example in aqueous solutions where both the polarity of the fluid and of the particles or cells can change the contact angle and wetting behavior dramatically. These contact angles mimic those discussed in the progression of phagocytosis and can play a critical role in particle shape and removal of the particle from circulation.

➔ Design Rule #1: Elongated filaments or particles with more complex geometries that achieve larger contact angles are beneficial because they avoid clearance by phagocytosis.

3.1.2 Phagocytosis: The impact of particle surface chemistry

An additional consideration to prevent recognition and clearance by macrophages includes the established strategy of decorating the particles with poly(ethylene) glycol (PEG), a hydrophilic polymer that shields the particles from opsonization [48] (see also Design Rule #3).

3.2 The impact of surface chemistry on cellular fate

3.2.1 Balancing targeting and shielding ligands

Targeting The overall goal in drug delivery is to achieve cell targeting and tissue-specificity while avoiding avoid phagocytosis and accumulation in non-target organs. Current developments in nanomedicine focus on receptor-mediated endocytosis (RME) to achieve the tissue-specific cellular delivery of nanoparticles. Antibodies or peptide ligands

specific for receptors overexpressed selectively on diseased cells are frequently used as surface ligands to confer tissue/cell-specificity. Many reports demonstrate the versatility of nanoparticle targeting strategies, several of which have been applied to virus-based materials. To name a few examples, CPMV nanoparticles have been targeted to vascular endothelial growth factor receptors and gastrin-releasing peptide receptors, both of which are known to be upregulated on tumor cells and tumor endothelium. Receptor targeting was achieved using short peptide sequences specific for these receptors. Tumor homing with targeted CPMV nanoparticles has been demonstrated using a mouse model of colon cancer [49] and an avian model of prostate cancer (Fig. 3) [50]. A popular targeting ligand is the RGD motif, which has been linked to CPMV, TMV, M13, and adeno-associated virus (AAV) vectors [33, 51–54]. Other targeting strategies include the use of ligands that naturally accumulate in tumor tissues, such as the iron-storage protein transferrin and vitamin folic acid. Proliferating cancer cells overexpress receptors for these ligands so the conjugation and multivalent display of transferrin or folic acid on the VNP surface promotes cancer cell targeting and uptake via endocytosis (Fig. 3). This has been demonstrated using MS2, CPMV, CPV, HCSRV, bacteriophage HK97, and several other viruses as well as other nanomaterials [30, 55–59].

➔ Design Rule #2: Receptor-specific ligands can be used to target specific cell types and enhance cellular uptake via endocytosis.

Peptide libraries and phage display technology enable us to identify targeting ligands specific for a particular receptor. Using such molecular biology screening tools, peptides with high selectively and affinity can be selected. Oftentimes, however, the fundamental interactions that play a role and trigger target specificity are not yet understood on a molecular level, and this thus presents another opportunity for improvements in nanomedical engineering. Some of these effects may arise due to the polar (acid/base) interactions that play important roles in nanoscale chemical interactions among systems in which covalent bonds are not formed.

Shielding Targeted cargo-delivery not only requires efficient uptake into target cells but also shielding from non-target cells, which can be achieved using dual modifications. For example, PEG chains are typically used to reduce the non-specific uptake and targeting ligands are used on the same particles to confer tissue-specificity, resulting in VNPs that can achieve immune evasion and efficient gene-delivery (Fig. 4) [59, 60].

➔ Design Rule #3: PEG or other shielding ligands should be included in the design to reduce non-specific cell interactions and evade the immune system.

3.2.2 Cell interactions depend on nanoparticle surface charge

Mammalian cell membranes are negatively charged because of their abundant proteoglycans. Nanomaterials therefore interact more strongly with mammalian cells if they are positively charged [61–63]. Strategies to enhance cell binding therefore include the use of positively charged poly(Arg) peptides (as an alternative strategy or in addition to receptor-specific targeting ligands discussed above) [64]. For example, we showed that CPMV particles decorated with 40 poly(Arg) peptides are taken up by cells eight times more efficiently than native CPMV [65].

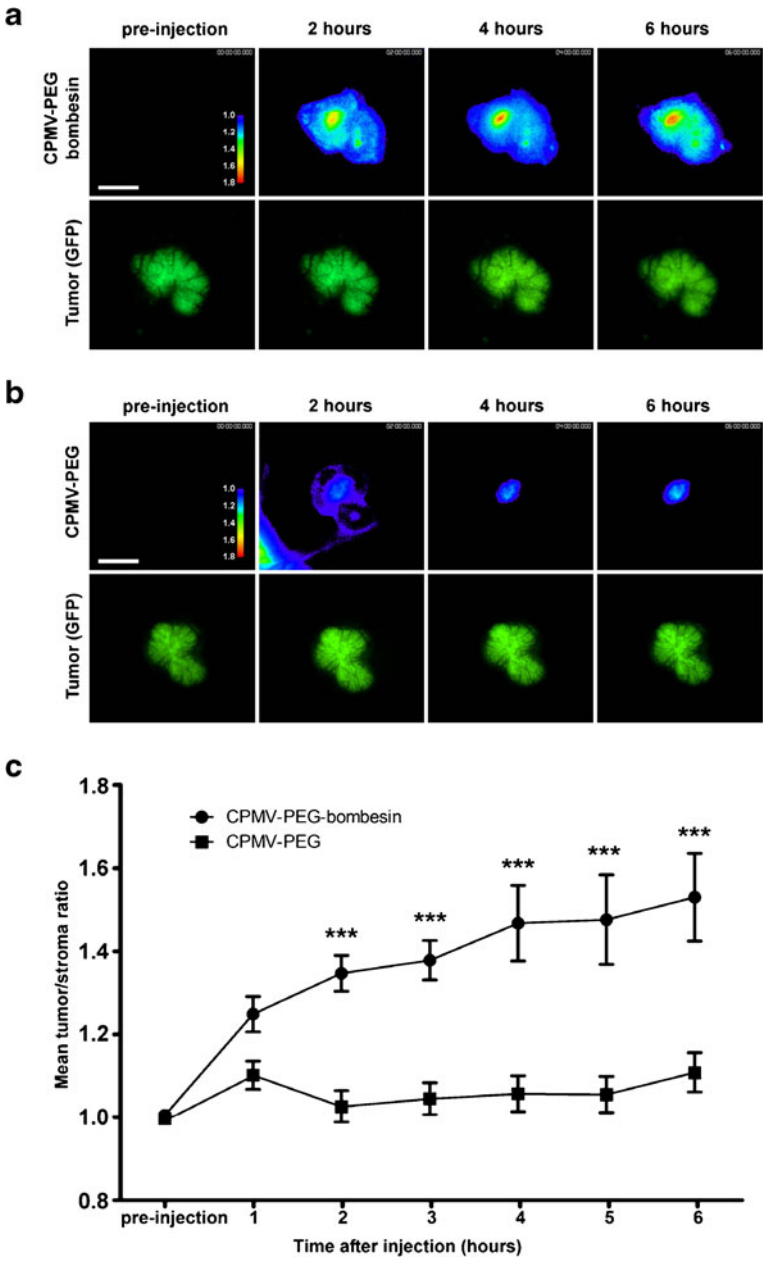

Fig. 3 Intravital imaging of viral nanoparticle uptake in prostate tumors in vivo. **a** Intravital fluorescence confocal imaging of PC-3 prostate tumor (*green channel*) showing uptake of AF647-labeled CPMV-PEG-BOMB (heat map) over time. Images are representative of $n = 10$ experiments. *Colors* correspond to tumor/stroma ratio (see key). *Scale bar* = 3 mm. **b** Intravital imaging of PC-3 prostate tumor (*green channel*) showing uptake of AF647-labeled CPMV-PEG (heat map) over time. Images are representative of $n = 10$ experiments. *Colors* correspond to tumor/stroma ratio (see key). *Scale bar* = 3 mm. **c** Quantitation of tumor uptake of CPMV conjugates over time, $n = 10$ experiments per group. Values expressed as mean tumor/stroma ratio, using GFP channel to delineate tumor. Uptake of CPMV-PEG-BOMB is significantly higher than CPMV-PEG ($P < 0.0001$). Reproduced with permission from Steinmetz et al., Small 2011 [50]

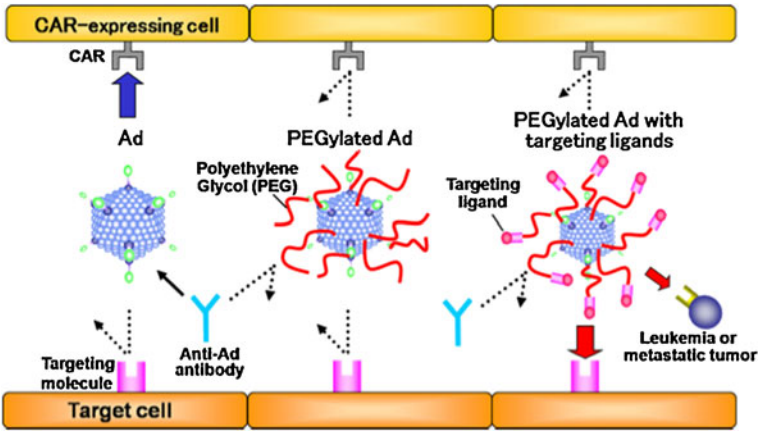

Fig. 4 Characteristics of PEGylated Ads. Non-modified Ads (*left panel*) bind to cells expressing the coxackie adenovirus receptor (CAR) and are recognized by neutralizing antibodies. PEGylated Ads (*middle panel*) do not bind to cells expressing CAR and are not recognized by neutralizing antibodies. These Ads, however, also do not bind to target cells. PEGylated Ads displaying targeting ligands on the periphery of the PEG chains are shielded from CAR expressing cells and antibodies. Targeting facilitates uptake by target cells and gene delivery. Reproduced with permission from Eto et al., Int J Pharm 2008 [60]

➔ Design Rule #4: Positively charged materials interact with mammalian cells more productively than negatively charged materials.

The Coulombic/electrostatic LRIs produce attractive and repulsive forces, have the longest range, and play substantial roles in biological processes [37]. At the same time, our understanding of these electrostatic interactions is limited to the mean-field Poisson–Boltzmann (PB) approximation, which in many situations does not agree with experimental observations. Even in simple electrostatic double layers, PB approaches are inadequate; electrostatic interactions of biological moieties in aqueous solutions demonstrate the limitations of our understanding. Also, with polyvalent cations, there can be attractive forces that are observed in osmotic stress measurements but are not present in PB calculations. So the simple design rule we cite has opportunity for refinement so as to illuminate how to use electrostatic interactions in the design and biomedical engineering process.

3.3 Receptor-mediated endocytosis of nanoparticles

3.3.1 Impact of particle size and ligand density on receptor-mediated endocytosis

We consider size and ligand density together because it is challenging to separate these variables. Mathematical models and molecular dynamics simulations have been developed using a simplistic representation of the cell membrane containing a single phospholipid and an excess of receptors exposed to different nanoparticle formulations to investigate factors that affect endocytosis, such as nanoparticle size and shape, binding strength, and ligand coverage [66]. Passive endocytosis occurs if there is a reduction in the free energy of the system, thus endocytosis increases with higher ligand coverage and receptor/ligand binding strength. This phenomenon can be explained using the Helfrich theory of membrane elasticity, in which spontaneous endocytosis can occur when the vesicle that ultimately

encapsulates the particle has a radius above a certain value that is dependent on membrane rigidity and mean membrane curvature [67].

These findings have been complemented using other mathematical models [68]. Minimum receptor density and minimum wrapping ratios can be determined, providing a basis for the rational engineering molecules that can be taken by endocytosis, because values below the minimum threshold will not provide sufficient energy to wrap the cell membrane around particle. The optimal particle radius was found to be a delicate balance between the thermodynamic driving force and the diffusion kinetics associated with the mobile receptor. While particles smaller than the optimal radius increased the total free energy, effectively inhibiting cell membrane wrapping, particles larger than the optimal radius could undergo wrapping although the process took longer because the receptors needed to diffuse over a greater distance (Fig. 5) [68].

These observations were experimentally verified using 50-nm transferrin-coated spherical gold nanoparticles, which were optimal for internalization by HeLa cells by clathrin-mediated endocytosis. The model did not predict that smaller particles would also be taken up by the cells, but this required a cluster to form prior to internalization [69]. Ultimately, modeling parameters such as the optimal particle radius, wrapping time, receptor density, and thermodynamic factors offer significant insight into the cellular dynamics that are contingent on receptor-mediated endocytosis.

➔ Design Rule #5: Multivalency and increased ligand density can enhance cellular uptake. Typically there is a threshold for optimal ligand density and spacing, which is highly dependent on the precise nature of the receptor–ligand system.

➔ Design Rule #6: The internalization process is dependent on the membrane wrapping time. Through competition between hydrodynamic driving force and receptor diffusion kinetics, there is an optimum radius (R* = 30–50 nm) for efficient wrapping [61, 62, 68, 70–75].

3.3.2 Impact of nanoparticle geometry on receptor-mediated endocytosis

Researchers have recently investigated the impact of particle shape on target cell binding and internalization. Although a growing body of data indicates that elongated filaments and

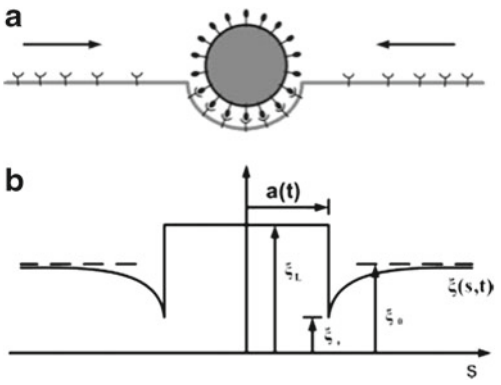

Fig. 5 Schematic illustration of the problem. **a** An initially flat membrane containing diffusive receptor molecules wraps around a ligand-coated particle. **b** The receptor density distribution in the membrane becomes nonuniform upon ligand-receptor binding; the receptor density is depleted in the near vicinity of the binding area and induces diffusion of receptors toward the binding site. Reproduced with permission from Gao et al., PNAS 2005 [68]

rods have superior pharmacokinetic and tumor-homing properties [45, 76–79], it is not yet clear how these materials interact with cells.

Models have shown that spherocylindrical particles are preferred over spherical particles for endocytosis, probably reflecting the lower mean curvature of the spherocylindrical particle. The orientation of the spherocylinders changed following uptake, such that they ultimately aligned in parallel with the membrane regardless of the initial orientation [66].

The effect of morphological anisotropy and initial orientation on particle penetration behavior was investigated using a dissipative particle dynamics models [80]. As found with phagocytosis, penetration became less efficient as the contact angle Ω increased for ellipsoids. Furthermore, the contact area and local curvature of the particle at the contact point also affected the efficiency of penetration across the lipid bilayer. Using discs with different radii, it was found that discs with smaller contact areas were better able to translocate as they caused less disruption to the packing states of the lipids in the bilayer. In addition, for particles such as ellipsoids whose curvature increases the disruption area during internalization, the necessary force for penetration is lower if the particles are longer, causing the change to be more gradual. Interestingly, the force required for penetration was greater for longer cylinders [80].

Whereas modeling allows the precise and individual control of geometry and surface chemistry, these labels are more difficult to separate in physical experiments. Although there are data showing that particle geometry does affect cellular uptake, a consensus has yet to be reached. For example, when gold nanorods and spheres are targeted to breast cancer cells, the particles with the highest aspect ratio are taken up more slowly. However, the nanorods were found to form aggregates in the culture medium, with longer rods forming larger aggregates that may be more difficult to take up [81]. Similar observations were made when comparing the internalization of transferrin-coated gold nanorods and spherical particles by cervical cancer cells. The rods were internalized much more slowly than the spheres, but the transferrin was concentrated at the ends of the rods, making receptor–ligand interactions more challenging [82].

Different results have been reported using cationic PEG hydrogel cylinders produced by PRINT (particle replication in nonwetting template) technology (Fig. 6) [63]. Here, higher aspect ratio cylinders were internalized more rapidly than isotropic cylinders with a similar volume by cervical cancer cells. The difference in material properties, e.g., charge, may play a role in these different behaviors. The impact of charge was investigated by treating the particles with acetic anhydride to convert surface amine groups into amides. There was very little uptake of these particles, which are essentially identical except for the negative charge [63].

Some studies indicate that elongated materials with the same volume but different aspect ratios have distinct internalization rates, with higher aspect ratios resulting in faster uptake kinetics [62, 63]. However, others have shown the opposite phenomenon, i.e., nanorods with a low aspect ratio are taken up more efficiently [83] and spheres interact more efficiently with cells than rods [82, 84, 85].

➔ Design Rule #7: Ellipsoid and cylindrical particles may be ideal for targeted uptake if the aspect ratio is optimized and especially if contact orientation can be controlled. Geometry plays a role in the efficiency of cellular uptake, but more research is required to define the design rule.

A potential avenue would be to include physics and fundamental LRIs into biological measurement and testing. From a physical point of view, anisotropy in nanoparticles can

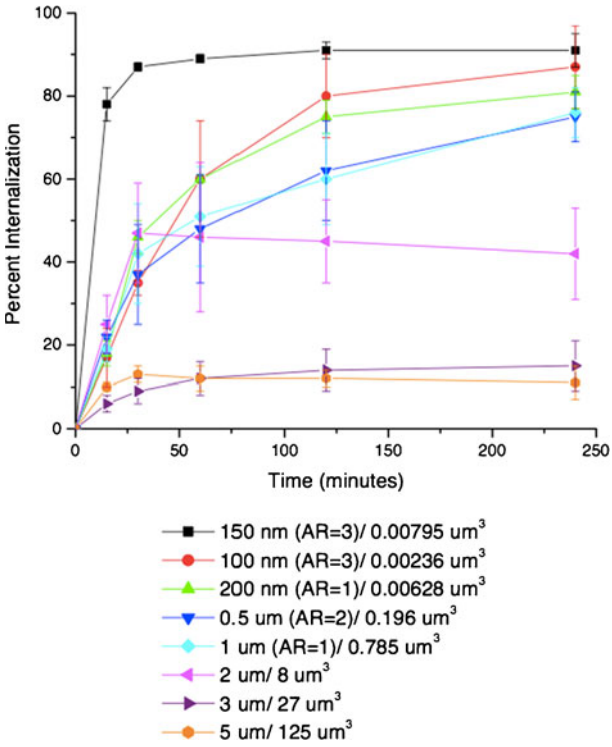

Fig. 6 Internalization profile of PRINT particles with HeLa cells over a 4-h incubation period at 37 °C. Legend depicts the particle diameter per particle volume. Reproduced with permission from Gratton et al. PNAS 2008 [63]

be morphological (shape), chemical, and/or optical [37]. Many biological materials show strong optical anisotropy, such as can be seen in fibrillar and helical materials. An example of both morphological and optical anisotropy is found in vdW–Ld interactions of carbon nanotubes (CNTs), in which optical anisotropy is observed for electric fields along, versus perpendicular to, the tube axis. In this case, one finds that there is both shape and optical anisotropy leading to not only attractive or repulsive normal force acting between CNTs in solutions but also giving rise to vdW–Ld torques, which can promote mutual alignment of CNTs in solution and upon deposition on surfaces [86]. These vdW–Ld torques are forces that can be manipulated for engineering purposes, and for example can allow optically anisotropic biological moieties to orient. Another example from CNTs is seen by single-stranded DNA, which wraps CNTs with a pitch that helps give net-charge to the DNA-CNT hybrids and enables the use of both vdW–Ld and electrostatic interactions for dispersion, separation, and placement of these hybrid moieties [87].

4 Nanoparticle–vascular interactions

4.1 Vascular targeting of nanoparticles

Understanding nanoparticle–cell interactions *in vitro* is the first step towards defining rules for the design of effective nanomedicines. However, studies under static conditions using monolayers of cells do not tell the whole story, and it is also necessary to consider interactions between nanoparticles and three-dimensional tissue models such as the vasculature under realistic flow conditions.

In vascular targeting, particles circulating in the vasculature must find the disease site on the endothelium, marginate to the vessel wall, adhere firmly to the endothelial cells, and then control whether they are internalized depending on the goal [88]. The margination of spherical, discoidal, ellipsoidal, and quasi-hemispherical silica particles in the microcirculation has been evaluated using a parallel plate flow chamber (Fig. 7) [76, 77]. Under linear laminar flow, non-spherical particles were more likely to drift laterally, and the lateral drift velocity was related to the Stokes number. Discoidal particles with low aspect ratios were more likely to marginate than other shapes in a gravitational field [76, 77].

Similar findings were reported in studies of liposomes, metallic gold, and iron oxide nanoparticles of various sizes and shapes, i.e., oblate particles showed a greater tendency for margination. In addition, smaller and less dense particles tended to marginate more efficiently, a trend that could be described by the inverse of a modified Peclet number [78].

The consistently superior margination of non-spherical particles reflects the fact that spherical particles tend to follow streamlines without lateral drift unless an external force is applied [89]. In contrast, non-spherical particles tend to rotate and tumble, thus resulting in lateral torque that causes margination without external forces [90]. Similar trends have been observed in other parts of the vasculature because red blood cells tend to congregate in the vessel cores, resulting in a cell-free layer close to the endothelial wall where nanoparticles travel in a linear laminar flow path [91]. This is advantageous because particles skimming the sides of larger vessels can marginate more readily and also leave larger vessels to enter the microcirculation [88].

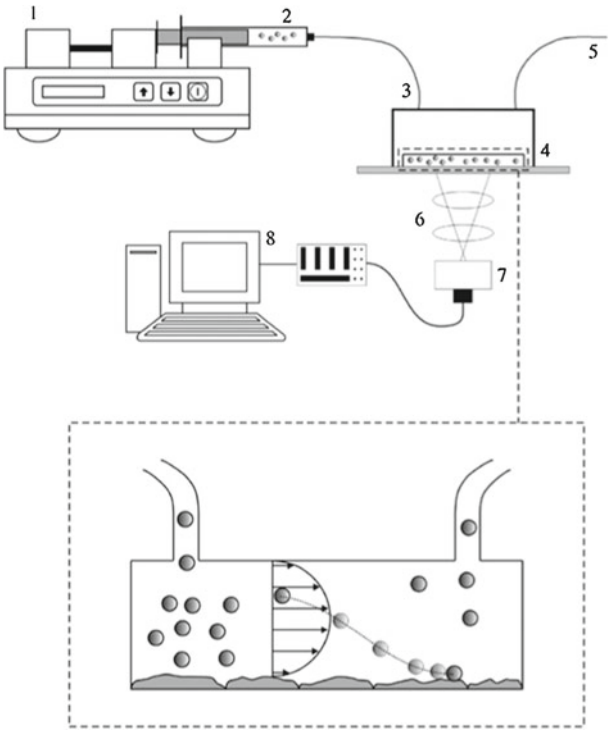

Fig. 7 A sketch of the experimental set-up comprising a syringe pump (1); a syringe with particles in solution (2); inlet Silastic tubing (3); a parallel plate flow chamber (4), outlet Silastic tubing (5); a microscope (6) with a digital camera (7) connected to a computer (8) for storage and imaging analysis. Reproduced with permission from Gentile at al. 2008, Journal of Biomechanics [77]

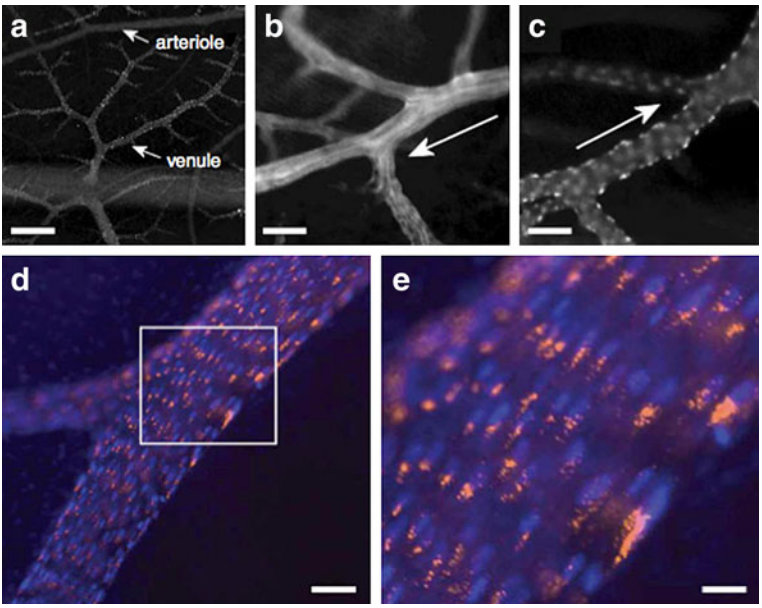

Fig. 8 Intravital fluorescence imaging of chick CAM vasculature and location of A555-labeled, fluorescent CPMV. **a** Fluorescence imaging looking down through surface chick CAM showing multiple levels of vasculature; *scale bar* is 100 μ. **b** CAM arteriole. *Scale bar* is 22 μ. **c** CAM venule; *scale bar* is 22 μ. *Arrows* in b and c denote blood flow direction. **d**, **e** Intravital image of large CAM vein, CPMV-A555 in *orange*, endothelial cells nuclei in *blue*. CPMV particles are restricted in the perinuclear compartment in vascular endothelial cells. *Scale bar* is 16 μ in **d** and 5.5. μ in **e**. Reproduced with permission from Lewis et al., Nature Medicine 2006 [95]

➔ Design Rule #8: Non-spherical, low-density nanoparticles have superior margination properties and thus a higher propensity to reach the target site.

Adhesion to target cells on the endothelium is necessary after margination. Firm adhesion occurs when dislodging forces and hydrodynamic shear stress at the vessel wall are overcome by non-specific adhesion forces and receptor–ligand interactions between the nanoparticles and the target cell. This requires a compromise in terms of size. As the particle size increases, more ligands are presented, offering more opportunities for the particles to interface with the endothelial cells, but the hydrodynamic forces also increase. This principle holds true for particles of various shapes, but oblate particles showed stronger cell adhesion than spherical particles for the same volume [92]. Following adhesion to the vascular target, and depending on the design, the particles may either remain in situ to serve as imaging contrast agents or may be internalized to release therapeutic agents.

➔ Design Rule #9: Oblate particles adhere more strongly to vascular targets.

➔ Design Rule #10: Size must be compromised: a larger nanoparticle has a larger surface area and can display more ligands that bind endothelial cells, but hydrodynamic and shear forces also increase with size and work against attachment.

4.2 CPMV—a nanoparticle with natural affinity for mammalian endothelial cells

Based on the design rules and physical phenomena described above, the currently favored 30-nm spherical VNP format may not be ideal for vascular targeting. However, research has shown that biology overwrites physics. CPMV has a natural affinity for vimentin [93, 94], a protein displayed on the surface of endothelial cells in the embryonic vasculature. Intravital imaging studies using fluorescence-labeled CPMV particles indicated that the plant VNP was specifically internalized by endothelial cells *in vivo* (Fig. 8) [95]. Vimentin is also overexpressed in tumor endothelium [96], which means CPMV is efficiently taken up into this tissue as shown using the chick chorioallantoic membrane tumor model. Fluorescence-labeled CPMV sensors accumulated within the tumor endothelium and allowed mapping and imaging over long time periods [95]. CPMV could therefore be used as a natural endothelial probe to image vascular disease and may provide novel insights into the expression profile of vimentin on the cell surface.

➔ Design Rule #11: Modeling and *in vitro* testing may provide insights into the fate of nanoparticles, but in vivo studies must accompany such evaluations because biological principles are more complex than mathematical and physical models can predict.

5 Pharmacokinetics

5.1 Impact of nanoparticle shape on pharmacokinetic behavior

Another benefit of particle accumulation close to blood vessel walls is the enhanced permeability and retention (EPR) effect, which means nanoparticles can passively diffuse across the tumor endothelium due to the leaky vasculature and inefficient lymphatic drainage from tumor hypervascularization [97]. Longer circulation times and better margination properties therefore favor particle escape through fenestrations into the tumor microenvironment. Not surprisingly, circulation time is also influenced by particle shape. For example, filomicelles last up to ten times longer and therefore possess superior tumor-targeting properties compared to spherical micelles, probably due to the evasion of phagocytosis (see design rule #1) [45]. Furthermore, PEG linkers can be incorporated to reduce macrophage recognition, therefore increasing both active and passive targeting efficiency by extending the circulation time [98, 99].

➔ Design Rule #12: Elongated materials have longer circulation times and enhanced tumor-homing properties compared to spherical nanoparticles.

5.2 Impact of nanoparticle surface charge on pharmacokinetic behavior

Surface charges of the nanocarrier play a role in electrostatic interactions with circulating proteins and cells. Data indicate that positively charged nanomaterials have superior pharmacokinetic properties because they have longer plasma circulation times. In the case of VNPs, this means that negatively charged viruses such as CPMV and CCMV have rather short plasma circulation times ($t_{1/2} < 15$ min) [18, 19], whereas positively charged viruses such as bacteriophage Qβ are much more persistent ($t_{1/2} = 3$ h) [100]. VNPs can be genetically or chemically modified to increase the number of positively charged amino acid residues, and regardless of the platform (e.g., Qβ, λ, and M13), the circulation time increased in line with the number of additional positive charges [100–103].

➔ Design Rule #13: Positively charged materials have longer circulation times.

When considering VNPs, one must keep in mind that even though the net charge may be negative or positive, VNPs are biological entities that consist of complex patterns of amino acids of varying charges in the local microenvironment of the capsid. Two VNPs of comparable net surface charge (or zeta potential) may or may not have similar pharmacokinetics. The local charge distribution may impact the interactions with plasma proteins.

In physics, grading of the interfacial properties, such as charge and composition, can also play a strong role in the formation and performance of interfaces over time. Graded interfaces are observed in many real systems, and are typically ignored in our modeling and design of systems. Yet these graded interfaces can themselves exhibit important thermodynamic free energies and better stability than abrupt interfaces that are typically idealized [37, 104, 105].

6 Nanoparticle transport in solid tumors

6.1 Impact of nanoparticle size on transport within solid tumors

In healthy tissues, the movement of molecules is driven by diffusion (concentration gradients) and convection (pressure gradients). In tumor tissues, the leaky vasculature and lack of a functional lymphatic drainage increases the interstitial fluid pressure [106], which reduces convective transport from the vessel wall into the interstitial space. Therefore, diffusion is the primary mode of nanoparticle and drug transport in tumor tissues. The diffusion coefficient correlates inversely with the hydrodynamic radius (R_H) of the nanoparticle (based on the Stokes–Einstein relationship); thus the smaller the material, the more efficient the diffusion. However, larger particles (60–100 nm) are more likely to accumulate in the tumor based on the EPR effect (Fig. 9) [107]. To meet both requirements, i.e., preferable larger size for tumor homing and preferable smaller size for enhanced penetration, a number of multistage delivery systems have been developed in which a complex of nanoparticles is used to navigate the vasculature to reach the target site, whereupon the structure disintegrates and releases smaller nanoparticles for enhanced tissue penetration [108–110].

➔ Design Rule #14: Larger nanoparticles are more likely to accumulate in the tumor or target the vessel wall (see Design Rules #9 and #10), but smaller particles can penetrate more deeply. Multistage delivery systems are therefore ideal to meet both requirements.

6.2 Impact of nanoparticle shape on transport within solid tumors

Filamentous rods have superior tumor-homing properties to spherical nanoparticles because of their longer circulation times and beneficial flow properties. Data also indicate that elongated materials are transported across plasma membranes more efficiently: nanorods (54 × 15 nm) with the same effective hydrodynamic radius and diffusive transport in water as nanospheres (35 nm) are more efficient at penetrating gels and tumor tissues [111]. The short, cross-sectional dimension of nanorods determines the membrane transfer efficiency [111].

We recently compared the biodistribution and tumor-homing properties of filamentous PVX (515 × 13 nm) and icosahedral CPMV (30 nm) particles. Both were decorated with fluorescent dyes for tracking and with PEG to reduce immunogenicity and nonspecific binding. Tumor-homing studies were carried out using avian embryo and athymic nude

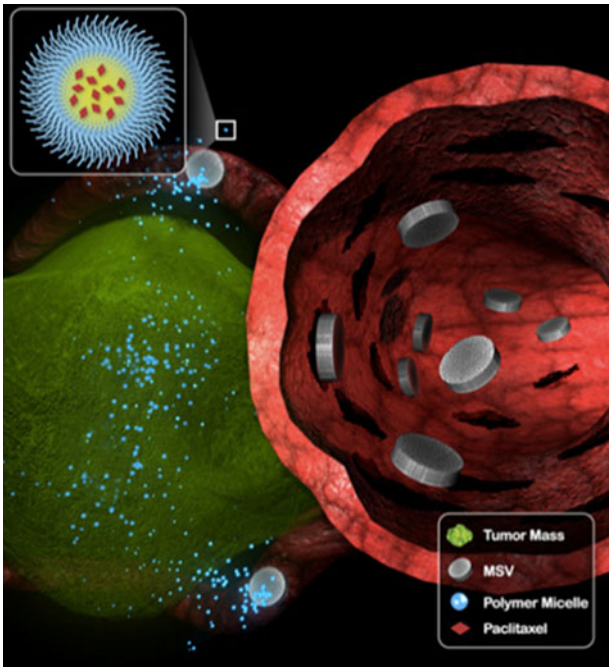

Fig. 9 Proposed mechanism of multistage delivery of micellar nanotherapeutics to tumors. Following navigation in blood vessels, multistage vectors (MSVs) marginate in tumor vasculature, accumulating in smaller capillaries. MSVs then become intravascular drug-delivery depots, releasing paclitaxel-containing polymer micelles in a sustained fashion over time. Reproduced with permission from Blanco et al., Cancer Letters, 2012 [108]

mouse tumor xenograft models of fibrosarcoma, squamous carcinoma, and colon cancer. The chick chorioallantoic membrane (CAM) model is convenient for the intravital imaging of angiogenesis and VNP uptake [95]. Using this model, we found that PVX accumulated to significantly higher levels in the tumor core compared to CPMV, confirming enhanced penetration into the tumor tissue. Furthermore, *ex vivo* imaging and fluorescence plate-reader assays in the mouse studies showed that PVX was more efficient at tumor homing than CPMV. The analysis of tumor sections showed that PVX penetrates tumors more effectively, confirming the results from the CAM model (Fig. 10) [95]. In addition to the advantageous shape of PVX, it is also positively charged, whereas CPMV is negatively charged (see Design Rule #16). Charge must be separated from shape to define a clear rule, and we are currently evaluating VNPs with different shapes and degrees of elasticity (stiff vs. flexible) but similar surface charges.

➔ Design Rule #15: Filamentous rods have superior tumor-homing properties and enhanced transport across plasma membranes.

6.3 Impact of nanoparticle surface charge on transport within solid tumors

Surface charge plays a central role in protein–protein interactions, cellular interactions, and pharmacokinetics. Not surprisingly, surface charge also affects the transport of nanomaterials within tissues: positively charged materials penetrate tissues and accumulate within them more efficiently than negatively charged materials. The collagen-rich matrix is a major determinant of interstitial transport [112]. Collagen carries a positive charge, and negatively charged materials can aggregate in the collagen matrix through electrostatic

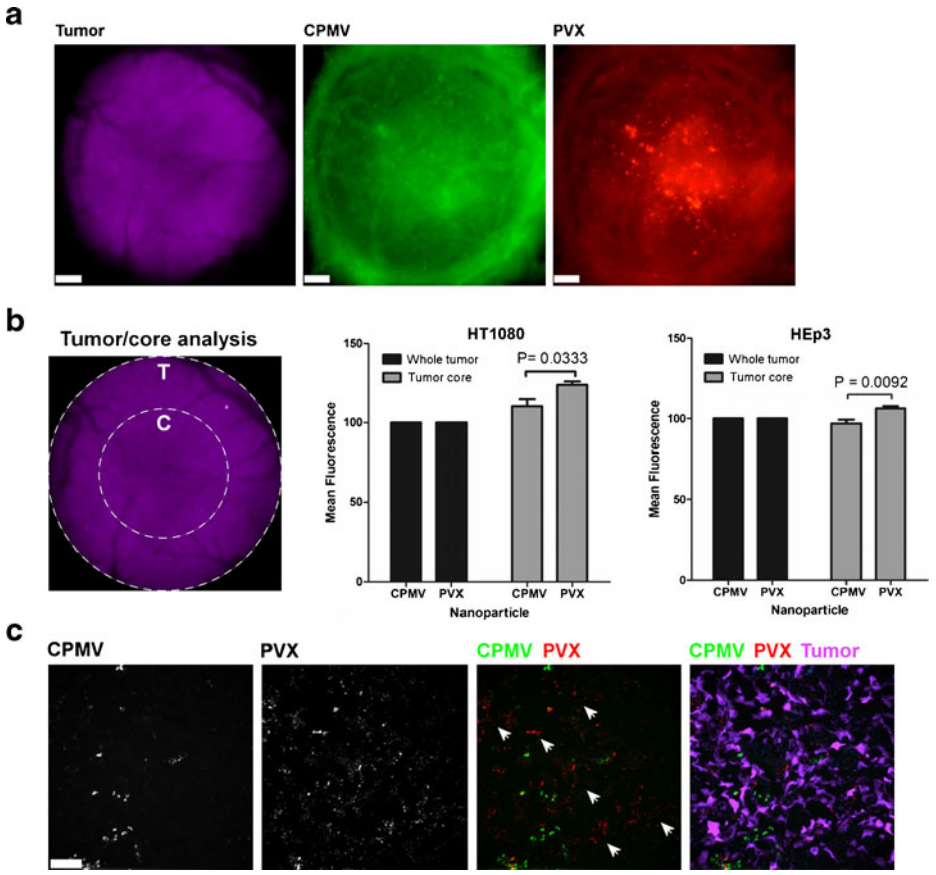

Fig. 10 Intravital imaging of VNP uptake in human tumor xenografts in the CAM. **a** Avian embryos bearing vascularized GFP-expressing human fibrosarcoma HT1080 or human epithelial carcinoma HEp3 tumors (*magenta*) were co-injected with 515 × 13 nm filamentous PVX-PEG-A555 (*red*) and 30 nm-sized icosahedron CPMV-PEG-647 (*green*) and visualized 4 h after injection. *Scale bar* = 190 μm. **b** The analysis of whole tumor uptake of CPMV and PVX nanoparticles compared to uptake only in the tumor core was assessed using distinct ROIs (*left panel*) in HT1080 (*middle panel*) and HEp3 (*right panel*) tumors. While whole tumor localization of CPMV and PVX were comparable, PVX accumulated in the core of tumors to a significantly higher degree than CPMV (unpaired *t* test). **c** The localization of nanoparticles was assessed in 8 μ sections of the tumor core using fluorescence microscopy. CPMV (*green*) and PVX (*red*) are visualized in the tumor (*magenta*). While CPMV was visualized in punctate foci, PVX was distributed throughout the tumor in areas devoid of CPMV (*white arrowheads*). Reproduced with permission from Shukla et al., Mol. Pharm. 2013 [95]

interactions, thus limiting their diffusion rates. Cationic nanoparticles have enhanced tumor-homing properties and also exhibit higher vascular permeability compared to their anionic counterparts [113–117].

➔ Design Rule #16: Positively charged materials have enhanced tumor-transport rates.

Considering transport in tumor tissue, various nanoparticle parameters play a role, including size, shape, and surface chemistry/charge. One must also keep in mind that tumors are heterogeneous structures consisting of different cell types, and the connecting

tissue throughout the diseased area can have varying degrees of density and other structural properties. The interfacial layer between the tumor and the nanoparticle is the last hurdle to overcome and plays a role with great importance. If drugs are not distributed efficiently and cells are treated with sublethal doses, this can trigger development of drug resistance and/or reoccurrence of the disease in a more aggressive form. In physics, interfacial films that serve a lubricant role can be designed to appear at interfaces [118, 119]. If a similar approach could be produced in response to the solid tumor environment, then tumor penetration would be improved.

7 Summary and outlook

Nanosciences and technology have revolutionized medicine, and significant advances have been made in disease detection, imaging, and treatment. Delivery vehicles have been designed, developed, and tested that show promising results in the laboratory as well as in the clinic. Targeted drug delivery, as an example, allows for the increase of the local concentration of the drug at the target site, thus increasing efficacy while at the same time reducing adverse effects, representing an important milestone in chemotherapy treatment for cancer patients.

As the research field of nanotechnology grows, rules guiding the intelligent design of delivery vehicles are emerging (Table 1). More research is required to fully comprehend the rules and allow for global optimization. Early research focused on the study of surface chemistry of nanoparticles, and PEGylation was defined as a successful strategy to reduce undesired nanoparticle–protein and –cell interactions, thereby improving pharmacokinetic stability and biodistribution. More recent research has focused on the study how physical properties, such as nanoparticle size and shape, impact their *in vivo* fate as they circulate and are delivered to the tumor. Based on abundance and ease of synthesis of spherical nanomaterials, most research and (pre)clinical testing has focused on the study of spherical particles, such as liposomes, dendrimers, and icosahedral VNPs. However, recent data indicate advantages of non-spherical materials, and this suggests a paradigm shift in nanomedical engineering. Advances in nanomanufacturing and chemical synthesis can assist with the production of nanomaterials of diverse shapes and compositions tailored for specific applications. An emerging trend is the development of multistage systems, in which specialized materials and components are linked together to navigate the body's complex systems so as to deliver cargos to specific cells, tissues, and/or organs.

The application of VNPs as delivery systems for imaging and/or drug delivery is still a young discipline; only a few VNP structures have been studied in pre-clinical animal models. Given the diverse shapes and sizes of genetically controlled and monodispersed VNP systems provided by nature (Fig. 1), we can explore and potentially exploit the more exotic structures, rather than solely focusing our efforts on the traditional viral icosahedron. Advances in physical virology, along with development of protocols and methods that allow tailoring of VNPs via genetic and chemical modification, provide a foundation to apply engineering concepts to a variety of structures. Our lab has turned toward structure–function studies with the goal to further elucidate how shape, aspect ratio, charge, and flexibility of VNP carriers impact their *in vivo* fate. This is expected to help define rules for effective design of delivery vehicles for their ultimate clinical benefit. Based on these genetically controlled and monodispersed structures, in combination with design rule guidance, VNPs provide an exciting platform to define structure–function relationships in nanomedicine and to produce targeted delivery vehicles.

Table 1 Summary of design rules

#	Design rule
1	Elongated filaments or particles with more complex geometries that achieve larger contact angles can better avoid clearance by phagocytosis.
2	Receptor-specific ligands can be used to target specific cell types and enhance cellular uptake via endocytosis.
3	PEG or other shielding ligands should be included to reduce non-specific cell interactions and evade the immune system.
4	Positively charged materials interact with mammalian cells more productively than negatively charged materials.
5	Multivalency and increased ligand density can enhance cellular uptake, but typically there is a threshold for optimal ligand density and spacing.
6	Through competition between hydrodynamic driving force and receptor diffusion kinetics, there is an optimum radius ($R^* = 30–50$ nm) for efficient membrane wrapping and internalization.
7	Ellipsoid and cylindrical particles may be ideal for targeted uptake if the aspect ratio is optimized and especially if contact orientation can be controlled.
8	Non-spherical, low-density nanoparticles have superior margination properties and thus a higher propensity to reach the target site.
9	Oblate particles adhere more strongly to vascular targets.
10	Size must be compromised: a larger nanoparticle has a larger surface area and can display more ligands for binding, but hydrodynamic and shear forces are also greater and work against attachment.
11	*In vivo* studies must accompany modeling and *in vitro* testing because biological principles are more complex than mathematical and physical models can predict.
12	Elongated materials have longer circulation times and superior tumor homing properties compared to spherical nanoparticles.
13	Positively charged materials have longer circulation times.
14	Larger nanoparticles are more likely to accumulate in the tumor or target the vessel wall, but smaller particles can penetrate more deeply.
15	Filamentous rods have superior tumor homing properties and enhanced transport across plasma membranes.
16	Positively charged materials have enhanced tumor transport rates.

Nanomedicine, including the branch of VNPs, is an interdisciplinary research effort: physical virology lays the foundation and provides knowledge in virus structure and assembly. Developments in chemistry produce manifold protocols and methods for tailoring of VNPs. Biology and bio(medical) engineering contribute to the fundamental understanding of the *in vivo* properties of VNP-based materials and to their ultimate development and implementation.

Biophysical modeling and experiments will provide the basis to integrate our knowledge of the fundamental LRIs dictating the lifecycle and fate of cargo-loaded VNPs in their changing environments, for example the plasma during circulation and the tumor tissue at the target site. Understanding these fundamental interactions will help not only the VNP design lab but also nanomedical engineers to develop clinically effective delivery systems.

Acknowledgements This work was supported by NIH/NIBIB grant R00 EB009105 (to NFS, for the contribution on virus-based nanomedicines and identification of design rules), NIH/NIBIB training grant T32 EB007509 (to AMW, for the contribution on virus-based nanomedicines), Mt. Sinai Foundation (to NFS, for the contribution on virus-based nanomedicines and identification of design rules), and DOE-BES-DMSE-BMM under award DE-SC0008068 (to RHF, for the contribution of role of long range interactions in self-assembly).

References

1. Longmire, M.R., Ogawa, M., Choyke, P.L., Kobayashi, H.: Biologically optimized nanosized molecules and particles: more than just size. Bioconjug. Chem. **22**, 993–1000 (2011)
2. Cheng, Z., Al Zaki, A., Hui, J.Z., Muzykantov, V.R., Tsourkas, A.: Multifunctional nanoparticles: cost versus benefit of adding targeting and imaging capabilities. Science **338**, 903–910 (2012)
3. Malik, N., Wiwattanapatapee, R., Klopsch, R., Lorenz, K., Frey, H., Weener, J.W., Meijer, E.W., Paulus, W., Duncan, R.: Dendrimers: relationship between structure and biocompatibility in vitro, and preliminary studies on the biodistribution of 125I-labelled polyamidoamine dendrimers in vivo. J. Control. Release **65**, 133–148 (2000)
4. Cheng, Y., Zhao, L., Li, Y., Xu, T.: Design of biocompatible dendrimers for cancer diagnosis and therapy: current status and future perspectives. Chem. Soc. Rev. **40**, 2673–2703 (2011)
5. Semmler-Behnke, M., Kreyling, W.G., Lipka, J., Fertsch, S., Wenk, A., Takenaka, S., Schmid, G., Brandau, W.: Biodistribution of 1.4- and 18-nm gold particles in rats. Small **4**, 2108–2111 (2008)
6. Harashima, H., Hiraiwa, T., Ochi, Y., Kiwada, H.: Size-dependent liposome degradation in blood: in vivo/in vitro correlation by kinetic modeling. J. Drug Target. **3**, 253–261 (1995)
7. Harashima, H., Kume, Y., Yamane, C., Kiwada, H.: Kinetic modeling of liposome degradation in blood circulation. Biopharm. Drug Dispos. **14**, 265–270 (1993)
8. Zhou, J.G., Chen, Y.M.: Research on PEGylation of porcine prothrombin for improving biostability and reducing animal immunogenicity. Bioorg. Med. Chem. Lett. **21**, 3268–3272 (2011)
9. Park, J.B., Kwon, Y.M., Lee, T.Y., Brim, R., Ko, M.C., Sunahara, R.K., Woods, J.H., Yang, V.C.: PEGylation of bacterial cocaine esterase for protection against protease digestion and immunogenicity. J. Control. Release **142**, 174–179 (2010)
10. Basu, A., Yang, K., Wang, M., Liu, S., Chintala, R., Palm, T., Zhao, H., Peng, P., Wu, D., Zhang, Z., Hua, J., Hsieh, M.C., Zhou, J., Petti, G., Li, X., Janjua, A., Mendez, M., Liu, J., Longley, C., Mehlig, M., Borowski, V., Viswanathan, M., Filpula, D.: Structure-function engineering of interferon-beta-1b for improving stability, solubility, potency, immunogenicity, and pharmacokinetic properties by site-selective mono-PEGylation. Bioconjug. Chem. **17**, 618–630 (2006)
11. Yang, Z., Wang, J., Lu, Q., Xu, J., Kobayashi, Y., Takakura, T., Takimoto, A., Yoshioka, T., Lian, C., Chen, C., Zhang, D., Zhang, Y., Li, S., Sun, X., Tan, Y., Yagi, S., Frenkel, E.P., Hoffman, R.M.: PEGylation confers greatly extended half-life and attenuated immunogenicity to recombinant methioninase in primates. Cancer Res. **64**, 6673–6678 (2004)
12. O'Riordan, C.R., Lachapelle, A., Delgado, C., Parkes, V., Wadsworth, S.C., Smith, A.E., Francis, G.E.: PEGylation of adenovirus with retention of infectivity and protection from neutralizing antibody in vitro and in vivo. Hum. Gene Ther. **10**, 1349–1358 (1999)
13. Raja, K.S., Wang, Q., Gonzalez, M.J., Manchester, M., Johnson, J.E., Finn, M.G.: Hybrid virus-polymer materials. 1. Synthesis and properties of PEG-decorated cowpea mosaic virus. Biomacromolecules **3**, 472–476 (2003)
14. Chitale, R.: Merck hopes to extend Gardasil vaccine to men. J. Natl. Cancer Inst. **101**, 222–223 (2009)
15. Liu, T.C., Galanis, E., Kirn, D.: Clinical trial results with oncolytic virotherapy: a century of promise, a decade of progress. Nat. Clin. Pract. Oncol. **4**, 101–117 (2007)
16. Shirakawa, T.: Clinical trial design for adenoviral gene therapy products. Drug News Perspect. **22**, 140–145 (2009)
17. Manchester, M., Singh, P.: Virus-based nanoparticles (VNPs): platform technologies for diagnostic imaging. Adv. Drug Deliv. Rev. **58**, 1505–1522 (2006)
18. Kaiser, C.R., Flenniken, M.L., Gillitzer, E., Harmsen, A.L., Harmsen, A.G., Jutila, M.A., Douglas, T., Young, M.J.: Biodistribution studies of protein cage nanoparticles demonstrate broad tissue distribution and rapid clearance in vivo. Int. J. Nanomedicine **2**, 715–733 (2007)
19. Singh, P., Prasuhn, D., Yeh, R.M., Destito, G., Rae, C.S., Osborn, K., Finn, M.G., Manchester, M.: Biodistribution, toxicity and pathology of cowpea mosaic virus nanoparticles in vivo. J. Control. Release **120**, 41–50 (2007)
20. Green, N.K., Herbert, C.W., Hale, S.J., Hale, A.B., Mautner, V., Harkins, R., Hermiston, T., Ulbrich, K., Fisher, K.D., Seymour, L.W.: Extended plasma circulation time and decreased toxicity of polymer-coated adenovirus. Gene Ther. **11**, 1256–1263 (2004)
21. Prangishvili, D., Forterre, P., Garrett, R.A.: Viruses of the Archaea: a unifying view. Nat. Rev. Microbiol. **4**, 837–848 (2006)
22. Rachel, R., Bettstetter, M., Hedlund, B.P., Haring, M., Kessler, A., Stetter, K.O., Prangishvili, D.: Remarkable morphological diversity of viruses and virus-like particles in hot terrestrial environments. Arch. Virol. **147**, 2419–2429 (2002)

23. Anderson, E.A., Isaacman, S., Peabody, D.S., Wang, E.Y., Canary, J.W., Kirshenbaum, K.: Viral nanoparticles donning a paramagnetic coat: conjugation of MRI contrast agents to the MS2 capsid. Nano Lett. **6**, 1160–1164 (2006)
24. Hooker, J.M., Datta, A., Botta, M., Raymond, K.N., Francis, M.B.: Magnetic resonance contrast agents from viral capsid shells: a comparison of exterior and interior cargo strategies. Nano Lett. **7**, 2207–2210 (2007)
25. Hooker, J.M., O'Neil, J.P., Romanini, D.W., Taylor, S.E., Francis, M.B.: Genome-free viral capsids as carriers for positron emission tomography radiolabels. Mol. Imaging Biol. **10**, 182–191 (2008)
26. Kovacs, E.W., Hooker, J.M., Romanini, D.W., Holder, P.G., Berry, K.E., Francis, M.B.: Dual-surface-modified bacteriophage MS2 as an ideal scaffold for a viral capsid-based drug delivery system. Bioconjug. Chem. **18**, 1140–1147 (2007)
27. Loo, L., Guenther, R.H., Lommel, S.A., Franzen, S.: Encapsidation of nanoparticles by red clover necrotic mosaic virus. J. Am. Chem. Soc. **129**, 11111–11117 (2007)
28. Loo, L., Guenther, R.H., Lommel, S.A., Franzen, S.: Infusion of dye molecules into Red clover necrotic mosaic virus. Chem. Commun. (Camb.) 88–90 (2008)
29. Ren, Y., Wong, S.M., Lim, L.Y.: In vitro-reassembled plant virus-like particles for loading of polyacids. J. Gen. Virol. **87**, 2749–2754 (2006)
30. Ren, Y., Wong, S.M., Lim, L.Y.: Folic acid-conjugated protein cages of a plant virus: a novel delivery platform for doxorubicin. Bioconjug. Chem. **18**, 836–843 (2007)
31. Suci, P.A., Berglund, D.L., Liepold, L., Brumfield, S., Pitts, B., Davison, W., Oltrogge, L., Hoyt, K.O., Codd, S., Stewart, P.S., Young, M., Douglas, T.: High-density targeting of a viral multifunctional nanoplatform to a pathogenic, biofilm-forming bacterium. Chem. Biol. **14**, 387–398 (2007)
32. Suci, P.A., Varpness, Z., Gillitzer, E., Douglas, T., Young, M.: Targeting and photodynamic killing of a microbial pathogen using protein cage architectures functionalized with a photosensitizer. Langmuir **23**, 12280–12286 (2007)
33. Bruckman, M.A., Kaur, G., Lee, L.A., Xie, F., Sepulveda, J., Breitenkamp, R., Zhang, X., Joralemon, M., Russell, T.P., Emrick, T., Wang, Q.: Surface modification of tobacco mosaic virus with "click" chemistry. ChemBioChem **9**, 519–523 (2008)
34. Steinmetz, N.F., Mertens, M.E., Taurog, R.E., Johnson, J.E., Commandeur, U., Fischer, R., Manchester, M.: Potato virus X as a novel platform for potential biomedical applications. Nano Lett. **10**, 305–312 (2010)
35. Rong, J., Lee, L.A., Li, K., Harp, B., Mello, C.M., Niu, Z., Wang, Q.: Oriented cell growth on self-assembled bacteriophage M13 thin films. Chem. Commun. (Camb.) 5185–5187 (2008)
36. Souza, G.R., Molina, J.R., Raphael, R.M., Ozawa, M.G., Stark, D.J., Levin, C.S., Bronk, L.F., Ananta, J.S., Mandelin, J., Georgescu, M.M., Bankson, J.A., Gelovani, J.G., Killian, T.C., Arap, W., Pasqualini, R.: Three-dimensional tissue culture based on magnetic cell levitation. Nat. Nanotechnol. **5**, 291–296 (2010)
37. French, R., Parsegian, V., Podgornik, R., Rajter, R., Jagota, A., Luo, J., Asthagiri, D., Chaudhury, M., Chiang, Y., Granick, S., Kalinin, S., Kardar, M., Kjellander, R., Langreth, D., Lewis, J., Lustig, S., Wesolowski, D., Wettlaufer, J., Ching, W., Finnis, M., Houlihan, F., Von Lilienfeld, O., Van Oss, C., Zemb, T.: Long-range interactions in nanoscale science. Rev. Mod. Phys. **82**, 1887–1944 (2010)
38. Chandler, D.: Hydrophobicity: two faces of water. Nature **417**, 491 (2002)
39. Israelachvili, J.N.: Intermolecular and Surface Forces, 3rd edn. Academic Press, Waltham, MA (2011)
40. Yildiz, I., Shukla, S., Steinmetz, N.F.: Applications of viral nanoparticles in medicine. Curr. Opin. Biotechnol. **22**, 901–908 (2011)
41. Ackler, H., French, R., Chiang, Y.: Comparisons of Hamaker constants for ceramic systems with intervening vacuum or water: from force laws and physical properties. J. Colloid Interface Sci. **179**, 460–469 (1996)
42. Aderem, A., Underhill, D.M.: Mechanisms of phagocytosis in macrophages. Annu. Rev. Immunol. **17**, 593–623 (1999)
43. Albanese, A., Tang, P.S., Chan, W.C.: The effect of nanoparticle size, shape, and surface chemistry on biological systems. Annu. Rev. Biomed. Eng. **14**, 1–16 (2012)
44. Champion, J.A., Mitragotri, S.: Role of target geometry in phagocytosis. Proc. Natl. Acad. Sci. U.S.A. **103**, 4930–4934 (2006)
45. Geng, Y., Dalhaimer, P., Cai, S., Tsai, R., Tewari, M., Minko, T., Discher, D.E.: Shape effects of filaments versus spherical particles in flow and drug delivery. Nat. Nanotechnol. **2**, 249–255 (2007)
46. French, R.: Origins and applications of London dispersion forces and Hamaker constants in ceramics. J. Am. Ceram. Soc. **83**, 2117–2146 (2000)
47. French, R.H., Winey, K.I., Yang, M.K., Qiu, W.: Optical properties and van der Waals–London dispersion interactions of polystyrene determined by vacuum ultraviolet spectroscopy and spectroscopic ellipsometry. Aust. J. Chem. **60**, 251–263 (2007)

48. Moghimi, S.M., Hunter, A.C., Murray, J.C.: Nanomedicine: current status and future prospects. FASEB J. **19**, 311–330 (2005)
49. Brunel, F.M., Lewis, J.D., Destito, G., Steinmetz, N.F., Manchester, M., Stuhlmann, H., Dawson, P.E.: Hydrazone ligation strategy to assemble multifunctional viral nanoparticles for cell imaging and tumor targeting. Nano Lett. **10**, 1093–1097 (2010)
50. Steinmetz, N.F., Ablack, A.L., Hickey, J.L., Ablack, J., Manocha, B., Mymryk, J.S., Luyt, L.G., Lewis, J.D.: Intravital imaging of human prostate cancer using viral nanoparticles targeted to gastrin-releasing Peptide receptors. Small **7**, 1664–1672 (2011)
51. Hovlid, M.L., Steinmetz, N.F., Laufer, B., Lau, J.L., Kuzelka, J., Wang, Q., Hyypia, T., Nemerow, G.R., Kessler, H., Manchester, M., Finn, M.G.: Guiding plant virus particles to integrin-displaying cells. Nanoscale **4**, 3698–3705 (2012)
52. Pasqualini, R., Koivunen, E., Ruoslahti, E.: Alpha v integrins as receptors for tumor targeting by circulating ligands. Nat. Biotechnol. **15**, 542–546 (1997)
53. Hajitou, A., Trepel, M., Lilley, C.E., Soghomonyan, S., Alauddin, M.M., Marini, F.C., 3rd, Restel, B.H., Ozawa, M.G., Moya, C.A., Rangel, R., Sun, Y., Zaoui, K., Schmidt, M., von Kalle, C., Weitzman, M.D., Gelovani, J.G., Pasqualini, R., Arap, W.: A hybrid vector for ligand-directed tumor targeting and molecular imaging. Cell **125**, 385–398 (2006)
54. Souza, G.R., Christianson, D.R., Staquicini, F.I., Ozawa, M.G., Snyder, E.Y., Sidman, R.L., Miller, J.H., Arap, W., Pasqualini, R.: Networks of gold nanoparticles and bacteriophage as biological sensors and cell-targeting agents. Proc. Natl. Acad. Sci. U.S.A. **103**, 1215–1220 (2006)
55. Huang, R.K., Steinmetz, N.F., Fu, C.Y., Manchester, M., Johnson, J.E.: Transferrin-mediated targeting of bacteriophage HK97 nanoparticles into tumor cells. Nanomedicine (Lond.) **6**, 55–68 (2011)
56. Brown, W.L., Mastico, R.A., Wu, M., Heal, K.G., Adams, C.J., Murray, J.B., Simpson, J.C., Lord, J.M., Taylor-Robinson, A.W., Stockley, P.G.: RNA bacteriophage capsid-mediated drug delivery and epitope presentation. Intervirology **45**, 371–380 (2002)
57. Sen Gupta, S., Kuzelka, J., Singh, P., Lewis, W.G., Manchester, M., Finn, M.G.: Accelerated bioorthogonal conjugation: a practical method for the ligation of diverse functional molecules to a polyvalent virus scaffold. Bioconjug. Chem. **16**, 1572–1579 (2005)
58. Singh, P., Destito, G., Schneemann, A., Manchester, M.: Canine parvovirus-like particles, a novel nanomaterial for tumor targeting. J. Nanobiotechnol. **4**, 2 (2006)
59. Destito, G., Yeh, R., Rae, C.S., Finn, M.G., Manchester, M.: Folic acid-mediated targeting of cowpea mosaic virus particles to tumor cells. Chem. Biol. **14**, 1152–1162 (2007)
60. Eto, Y., Yoshioka, Y., Mukai, Y., Okada, N., Nakagawa, S.: Development of PEGylated adenovirus vector with targeting ligand. Int. J. Pharm. **354**, 3–8 (2008)
61. Arnida, Janát-Amsbury, M.M., Ray, A., Peterson, C.M., Ghandehari, H.: Geometry and surface characteristics of gold nanoparticles influence their biodistribution and uptake by macrophages. Eur. J. Pharm. Biopharm. **77**, 417–423 (2011)
62. Arnida, Malugin, A., Ghandehari, H.: Cellular uptake and toxicity of gold nanoparticles in prostate cancer cells: a comparative study of rods and spheres. J. Appl. Toxicol. **30**, 212–217 (2010)
63. Gratton, S.E.A., Ropp, P.A., Pohlhaus, P.D., Luft, J.C., Madden, V.J., Napier, M.E., DeSimone, J.M.: The effect of particle design on cellular internalization pathways. Proc. Natl. Acad. Sci. U.S.A. **105**, 11613–11618 (2008)
64. Hillaireau, H., Couvreur, P.: Nanocarriers' entry into the cell: relevance to drug delivery. Cell. Mol. Life Sci. **66**, 2873–2896 (2009)
65. Wu, Z., Chen, K., Yildiz, I., Dirksen, A., Fischer, R., Dawson, P.E., Steinmetz, N.F.: Development of viral nanoparticles for efficient intracellular delivery. Nanoscale **4**, 3567–3576 (2012)
66. Vacha, R., Martinez-Veracoechea, F.J., Frenkel, D.: Receptor-mediated endocytosis of nanoparticles of various shapes. Nano Lett. **11**, 5391–5395 (2011)
67. Helfrich, W.: Elastic properties of lipid bilayers: theory and possible experiments. Z. Naturforsch. C **28**, 693–703 (1973)
68. Gao, H., Shi, W., Freund, L.B.: Mechanics of receptor-mediated endocytosis. Proc. Natl. Acad. Sci. U.S.A. **102**, 9469–9474 (2005)
69. Chithrani, B.D., Ghazani, A.A., Chan, W.C.: Determining the size and shape dependence of gold nanoparticle uptake into mammalian cells. Nano Lett. **6**, 662–668 (2006)
70. Aoyama, Y., Kanamori, T., Nakai, T., Sasaki, T., Horiuchi, S., Sando, S., Niidome, T.: Artificial viruses and their application to gene delivery. Size-controlled gene coating with glycocluster nanoparticles. J. Am. Chem. Soc. **125**, 3455–3457 (2003)
71. Desai, M.P., Labhasetwar, V., Walter, E., Levy, R.J., Amidon, G.L.: The mechanism of uptake of biodegradable microparticles in Caco-2 cells is size dependent. Pharm. Res. **14**, 1568–1573 (1997)

72. Jiang, W., Kim, B.Y.S., Rutka, J.T., Chan, W.C.W.: Nanoparticle-mediated cellular response is size-dependent. Nat. Nanotechnol. **3**, 145–150 (2008)
73. Nakai, T., Kanamori, T., Sando, S., Aoyama, Y.: Remarkably size-regulated cell invasion by artificial viruses. Saccharide-dependent self-aggregation of glycoviruses and its consequences in glycoviral gene delivery. J. Am. Chem. Soc. **125**, 8465–8475 (2003)
74. Osaki, F., Kanamori, T., Sando, S., Sera, T., Aoyama, Y.: A quantum dot conjugated sugar ball and its cellular uptake. On the size effects of endocytosis in the subviral region. J. Am. Chem. Soc. **126**, 6520–6521 (2004)
75. Prabha, S., Zhou, W.Z., Panyam, J., Labhasetwar, V.: Size-dependency of nanoparticle-mediated gene transfection: studies with fractionated nanoparticles. Int. J. Pharm. **244**, 105–115 (2002)
76. Lee, S.-Y., Ferrari, M., Decuzzi, P.: Shaping nano-/micro-particles for enhanced vascular interaction in laminar flows. Nanotechnology **20**, 495101 (2009)
77. Gentile, F., Chiappini, C., Fine, D., Bhavane, R.C., Peluccio, M.S., Cheng, M.M.-C., Liu, X., Ferrari, M., Decuzzi, P.: The effect of shape on the margination dynamics of non-neutrally buoyant particles in two-dimensional shear flows. J. Biomech. **41**, 2312–2318 (2008)
78. Toy, R., Hayden, E., Shoup, C., Baskaran, H., Karathanasis, E.: The effects of particle size, density and shape on margination of nanoparticles in microcirculation. Nanotechnology **22**, 115101 (2011)
79. Christian, D.A., Cai, S., Garbuzenko, O.B., Harada, T., Zajac, A.L., Minko, T., Discher, D.E.: Flexible filaments for in vivo imaging and delivery: persistent circulation of filomicelles opens the dosage window for sustained tumor shrinkage. Mol. Pharm. **6**, 1343–1352 (2009)
80. Yang, K., Ma, Y.Q.: Computer simulation of the translocation of nanoparticles with different shapes across a lipid bilayer. Nat. Nanotechnol. **5**, 579–583 (2010)
81. Qiu, Y., Liu, Y., Wang, L., Xu, L., Bai, R., Ji, Y., Wu, X., Zhao, Y., Li, Y., Chen, C.: Surface chemistry and aspect ratio mediated cellular uptake of Au nanorods. Biomaterials **31**, 7606–7619 (2010)
82. Chithrani, B.D., Ghazani, A.A., Chan, W.C.W.: Determining the size and shape dependence of gold nanoparticle uptake into mammalian cells. Nano Lett. **6**, 662–668 (2006)
83. Nan, A., Bai, X., Son, S.J., Lee, S.B., Ghandehari, H.: Cellular uptake and cytotoxicity of silica nanotubes. Nano Lett. **8**, 2150–2154 (2008)
84. Chithrani, B.D., Chan, W.C.W.: Elucidating the mechanism of cellular uptake and removal of protein-coated gold nanoparticles of different sizes and shapes. Nano Lett. **7**, 1542–1550 (2007)
85. Schaeublin, N.M., Braydich-Stolle, L.K., Maurer, E.I., Park, K., MacCuspie, R.I., Afrooz, A.R., Vaia, R.A., Saleh, N.B., Hussain, S.M.: Does shape matter? Bioeffects of gold nanomaterials in a human skin cell model. Langmuir **28**, 3248–3258 (2012)
86. Rajter, R.F., French, R.H., Ching, W.Y., Podgornik, R., Parsegian, V.A.: Chirality-dependent properties of carbon nanotubes: electronic structure, optical dispersion properties, Hamaker coefficients and van der Waals–London dispersion interactions. RSC Adv. **3**, 823–842 (2013)
87. Rajter, R., French, R.H.: Van der Waals-London dispersion interaction framework for experimentally realistic carbon nanotube systems. Int. J. Mater. Res. **101**, 27–42 (2010)
88. Decuzzi, P., Pasqualini, R., Arap, W., Ferrari, M.: Intravascular delivery of particulate systems: does geometry really matter? Pharm. Res. **26**, 235–243 (2009)
89. Goldman, A.J., Cox, R.G., Brenner, H.: Slow viscous motion of a sphere parallel to a plane wall—I Motion through a quiescent fluid. Chem. Eng. Sci. **22**, 637–651 (1967)
90. Gavze, E., Shapiro, M.: Motion of inertial spheroidal particles in a shear flow near a solid wall with special application to aerosol transport in microgravity. J. Fluid Mech. **371**, 59–79 (1998)
91. Fåhræus, R., Lindqvist, T.: The viscosity of the blood in narrow capillary tubes. Am. J. Physiol. **96**, 562–568 (1931)
92. Decuzzi, P., Lee, S., Bhushan, B., Ferrari, M.: A theoretical model for the margination of particles within blood vessels. Ann. Biomed. Eng. **33**, 179–190 (2005)
93. Koudelka, K.J., Destito, G., Plummer, E.M., Trauger, S.A., Siuzdak, G., Manchester, M.: Endothelial targeting of cowpea mosaic virus via surface vimentin. PLoS Pathog. **81**, 1632–1640 (2009)
94. Koudelka, K.J., Rae, C.S., Gonzalez, M.J., Manchester, M.: Interaction between a 54-kiloDalton mammalian cell surface protein and cowpea mosaic virus. J. Virol. **81**, 1632–1640 (2007)
95. Lewis, J.D., Destito, G., Zijlstra, A., Gonzalez, M.J., Quigley, J.P., Manchester, M., Stuhlmann, H.: Viral nanoparticles as tools for intravital vascular imaging. Nat. Med. **12**, 354–360 (2006)
96. van Beijnum, J.R., Dings, R.P., van der Linden, E., Zwaans, B.M., Ramaekers, F.C., Mayo, K.H., Griffioen, A.W.: Gene expression of tumor angiogenesis dissected: specific targeting of colon cancer angiogenic vasculature. Blood **108**, 2339–2348 (2006)
97. Maeda, H., Wu, J., Sawa, T., Matsumura, Y., Hori, K.: Tumor vascular permeability and the EPR effect in macromolecular therapeutics: a review. J. Control. Release **65**, 271–284 (2000)

98. Park, J.H., von Maltzahn, G., Zhang, L., Derfus, A.M., Simberg, D., Harris, T.J., Ruoslahti, E., Bhatia, S.N., Sailor, M.J.: Systematic surface engineering of magnetic nanoworms for in vivo tumor targeting. Small **5**, 694–700 (2009)
99. von Maltzahn, G., Park, J.H., Agrawal, A., Bandaru, N.K., Das, S.K., Sailor, M.J., Bhatia, S.N.: Computationally guided photothermal tumor therapy using long-circulating gold nanorod antennas. Cancer Res. **69**, 3892–3900 (2009)
100. Prasuhn, D.E., Jr., Singh, P., Strable, E., Brown, S., Manchester, M., Finn, M.G.: Plasma clearance of bacteriophage Qbeta particles as a function of surface charge. J. Am. Chem. Soc. **130**, 1328–1334 (2008)
101. Molenaar, T.J., Michon, I., de Haas, S.A., van Berkel, T.J., Kuiper, J., Biessen, E.A.: Uptake and processing of modified bacteriophage M13 in mice: implications for phage display. Virology **293**, 182–191 (2002)
102. Srivastava, A.S., Kaido, T., Carrier, E.: Immunological factors that affect the in vivo fate of T7 phage in the mouse. J. Virol. Methods **115**, 99–104 (2004)
103. Vitiello, C.L., Merril, C.R., Adhya, S.: An amino acid substitution in a capsid protein enhances phage survival in mouse circulatory system more than a 1,000-fold. Virus Res. **114**, 101–103 (2005)
104. van Benthem, K., Tan, G., DeNoyer, L., French, R., Ruhle, M.: Local optical properties, electron densities, and London dispersion energies of atomically structured grain boundaries. Phys. Rev. Lett. **93**, 227201 (2004)
105. van Benthem, K., Tan, G., French, R.H., DeNoyer, L.K., Podgornik, R., Parsegian, V.A.: Graded interface models for more accurate determination of van der Waals–London dispersion interactions across grain boundaries. Phys. Rev. B **74**, 205110 (2006)
106. Jain, R.K.: Transport of molecules, particles, and cells in solid tumors. Annu. Rev. Biomed. Eng. **1**, 241–263 (1999)
107. Perrault, S.D., Walkey, C., Jennings, T., Fischer, H.C., Chan, W.C.: Mediating tumor targeting efficiency of nanoparticles through design. Nano Lett. **9**, 1909–1915 (2009)
108. Blanco, E., Sangai, T., Hsiao, A., Ferrati, S., Bai, L., Liu, X., Meric-Bernstam, F., Ferrari, M.: Multistage delivery of chemotherapeutic nanoparticles for breast cancer treatment. Cancer Lett. (2012). doi:10.1016/j.canlet.2012.07.027
109. Stylianopoulos, T., Wong, C., Bawendi, M.G., Jain, R.K., Fukumura, D.: Multistage nanoparticles for improved delivery into tumor tissue. Methods Enzymol. **508**, 109–130 (2012)
110. Wong, C., Stylianopoulos, T., Cui, J., Martin, J., Chauhan, V.P., Jiang, W., Popovic, Z., Jain, R.K., Bawendi, M.G., Fukumura, D.: Multistage nanoparticle delivery system for deep penetration into tumor tissue. Proc. Natl. Acad. Sci. U.S.A. **108**, 2426–2431 (2011)
111. Chauhan, V.P., Popovic, Z., Chen, O., Cui, J., Fukumura, D., Bawendi, M.G., Jain, R.K.: Fluorescent nanorods and nanospheres for real-time in vivo probing of nanoparticle shape-dependent tumor penetration. Angew. Chem. Int. Ed. Engl. **50**, 11417–11420 (2011)
112. Jain, R.K., Stylianopoulos, T.: Delivering nanomedicine to solid tumors. Nat. Rev. Clin. Oncol. **7**, 653–664 (2010)
113. Campbell, R.B., Fukumura, D., Brown, E.B., Mazzola, L.M., Izumi, Y., Jain, R.K., Torchilin, V.P., Munn, L.L.: Cationic charge determines the distribution of liposomes between the vascular and extravascular compartments of tumors. Cancer Res. **62**, 6831–6836 (2002)
114. Dellian, M., Yuan, F., Trubetskoy, V.S., Torchilin, V.P., Jain, R.K.: Vascular permeability in a human tumour xenograft: molecular charge dependence. Br. J. Cancer **82**, 1513–1518 (2000)
115. Schmitt-Sody, M., Strieth, S., Krasnici, S., Sauer, B., Schulze, B., Teifel, M., Michaelis, U., Naujoks, K., Dellian, M.: Neovascular targeting therapy: paclitaxel encapsulated in cationic liposomes improves antitumoral efficacy. Clin. Cancer Res. **9**, 2335–2341 (2003)
116. Stylianopoulos, T., Diop-Frimpong, B., Munn, L.L., Jain, R.K.: Diffusion anisotropy in collagen gels and tumors: the effect of fiber network orientation. Biophys. J. **99**, 3119–3128 (2010)
117. Stylianopoulos, T., Poh, M.Z., Insin, N., Bawendi, M.G., Fukumura, D., Munn, L.L., Jain, R.K.: Diffusion of particles in the extracellular matrix: the effect of repulsive electrostatic interactions. Biophys. J. **99**, 1342–1349 (2010)
118. Chiang, Y., Silverman, L., French, R., Cannon, R.: Thin glass film between ultrafine conductor particles in thick-film resistors. J. Am. Ceram. Soc. **77**, 1143–1152 (1994)
119. French, R., Mullejans, H., Jones, D., Duscher, G., Cannon, R., Ruhle, M.: Dispersion forces and Hamaker constants for intergranular films in silicon nitride from spatially resolved-valence electron energy loss spectrum imaging. Acta Mater. **46**, 2271–2287 (1998)